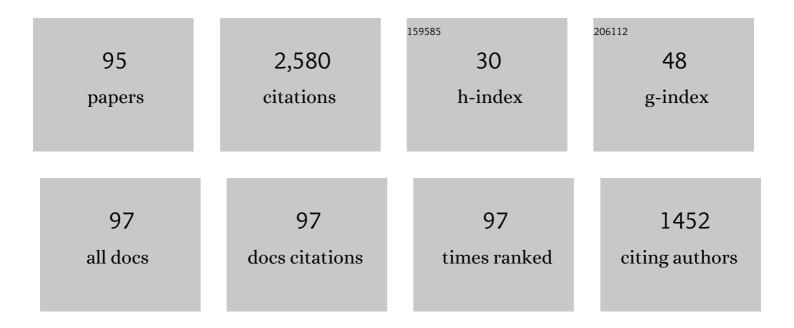
List of Publications by Year in descending order

Source: https://exaly.com/author-pdf/497940/publications.pdf Version: 2024-02-01



#	Article	IF	CITATIONS
1	Spark plasma sintering of transparent alumina. Scripta Materialia, 2007, 57, 607-610.	5.2	245
2	Microstructure and optical properties of transparent alumina. Acta Materialia, 2009, 57, 1319-1326.	7.9	160
3	Fabrication of transparent MgAl2O4 spinel polycrystal by spark plasma sintering processing. Scripta Materialia, 2008, 58, 1114-1117.	5.2	156
4	Effects of heating rate on microstructure and transparency of spark-plasma-sintered alumina. Journal of the European Ceramic Society, 2009, 29, 323-327.	5.7	154
5	Sparkâ€Plasmaâ€Sintering Condition Optimization for Producing Transparent MgAl ₂ O ₄ Spinel Polycrystal. Journal of the American Ceramic Society, 2009, 92, 1208-1216.	3.8	111
6	Spectroscopic study of the discoloration of transparent MgAl2O4 spinel fabricated by spark-plasma-sintering (SPS) processing. Acta Materialia, 2015, 84, 9-19.	7.9	88
7	Fabrication of Transparent Yttria by Highâ€Pressure Spark Plasma Sintering. Journal of the American Ceramic Society, 2011, 94, 3206-3210.	3.8	66
8	Reduction in sintering temperature for flash-sintering of yttria by nickel cation-doping. Acta Materialia, 2016, 106, 344-352.	7.9	64
9	Distribution of carbon contamination in oxide ceramics occurring during spark-plasma-sintering (SPS) processing: II - Effect of SPS and loading temperatures. Journal of the European Ceramic Society, 2018, 38, 2596-2604.	5.7	62
10	Optical Properties and Microstructure of Nanocrystalline Cubic Zirconia Prepared by Highâ€Pressure Spark Plasma Sintering. Journal of the American Ceramic Society, 2011, 94, 2981-2986.	3.8	58
11	Effect of sintering temperature on optical properties and microstructure of translucent zirconia prepared by high-pressure spark plasma sintering. Science and Technology of Advanced Materials, 2011, 12, 055003.	6.1	57
12	Fabrication of high-strength transparent MgAl ₂ O ₄ spinel polycrystals by optimizing spark-plasma-sintering conditions. Journal of Materials Research, 2009, 24, 2863-2872.	2.6	55
13	Effects of Preheating of Powder Before Spark Plasma Sintering of Transparent MgAl ₂ O ₄ Spinel. Journal of the American Ceramic Society, 2010, 93, 2158-2160.	3.8	54
14	Lowâ€Temperature Spark Plasma Sintering of Yttria Ceramics with Ultrafine Grain Size. Journal of the American Ceramic Society, 2011, 94, 3301-3307.	3.8	54
15	Densification behavior of a fine-grained MgAl2O4 spinel during spark plasma sintering (SPS). Scripta Materialia, 2010, 63, 565-568.	5.2	52
16	Influence of pre- and post-annealing on discoloration of MgAl2O4 spinel fabricated by spark-plasma-sintering (SPS). Journal of the European Ceramic Society, 2016, 36, 2961-2968.	5.7	49
17	High-pressure spark plasma sintering of MgO-doped transparent alumina. Journal of the Ceramic Society of Japan, 2012, 120, 116-118.	1.1	48
18	Enhanced superplasticity in a alumina-containing zirconia prepared by colloidal processing. Scripta Materialia, 2000, 43, 705-710.	5.2	47

#	Article	IF	CITATIONS
19	Densification of Nanocrystalline Yttria by Low Temperature Spark Plasma Sintering. Journal of the American Ceramic Society, 2008, 91, 1707-1710.	3.8	46
20	Influence of Spark Plasma Sintering (<scp>SPS</scp>) Conditions on Transmission of MgAl ₂ O ₄ Spinel. Journal of the American Ceramic Society, 2015, 98, 378-385.	3.8	44
21	Distribution of carbon contamination in MgAl2O4 spinel occurring during spark-plasma-sintering (SPS) processing: I – Effect of heating rate and post-annealing. Journal of the European Ceramic Society, 2018, 38, 2588-2595.	5.7	43
22	High-strain-rate superplasticity in oxide ceramics. Science and Technology of Advanced Materials, 2007, 8, 578-587.	6.1	41
23	Effect of Alumina Dopant on Transparency of Tetragonal Zirconia. Journal of Nanomaterials, 2012, 2012, 1-5.	2.7	41
24	Synthesis of dense nanocrystalline ZrO2–MgAl2O4 spinel composite. Scripta Materialia, 2005, 53, 1007-1012.	5.2	39
25	Effect of loading schedule on densification of MgAl2O4 spinel during spark plasma sintering (SPS) processing. Journal of the European Ceramic Society, 2012, 32, 2303-2309.	5.7	37
26	Assessment of carbon contamination in MgAl ₂ 0 ₄ spinel during spark-plasma-sintering (SPS) processing. Journal of the Ceramic Society of Japan, 2015, 123, 983-988.	1.1	37
27	Transparent ultrafine Yb ³⁺ :Y ₂ O ₃ laser ceramics fabricated by spark plasma sintering. Journal of the American Ceramic Society, 2018, 101, 694-702.	3.8	37
28	Highâ€Strainâ€Rate Superplasticity in Y ₂ O ₃ â€Stabilized Tetragonal ZrO ₂ Dispersed with 30 vol% MgAl ₂ O ₄ Spinel. Journal of the American Ceramic Society, 2002, 85, 1900-1902.	3.8	36
29	Effect of minor SiO2 addition on the creep behavior of superplastic tetragonal ZrO2. Acta Materialia, 2004, 52, 3355-3364.	7.9	35
30	Kinetics of Normal Grain Growth Depending on the Size Distribution of Small Grains. Materials Transactions, 2003, 44, 2239-2244.	1.2	32
31	Highly Infrared Transparent Nanometric Tetragonal Zirconia Prepared by Highâ€Pressure Spark Plasma Sintering. Journal of the American Ceramic Society, 2011, 94, 2739-2741.	3.8	27
32	Evolution of microstructure, mechanical, and optical properties of Y2O3-MgO nanocomposites fabricated by high pressure spark plasma sintering. Journal of the European Ceramic Society, 2020, 40, 4547-4555.	5.7	25
33	Electric current dependence of plastic flow behavior with large tensile elongation in tetragonal zirconia polycrystal under a DC field. Scripta Materialia, 2021, 194, 113659.	5.2	24
34	Densification kinetics during isothermal sintering of 8YSZ. Journal of the European Ceramic Society, 2016, 36, 1269-1275.	5.7	22
35	Reply to "Comment on the role of intragranular dislocations in superplastic yttria-stabilized zirconia― Scripta Materialia, 2003, 48, 1403-1407.	5.2	20
36	Microstructural Design for High-Strain-Rate Superplastic Oxide Ceramics. Journal of the Ceramic Society of Japan, 2005, 113, 191-197.	1.3	20

#	Article	lF	CITATIONS
37	Synthesis of highly-infrared transparent Y2O3–MgO nanocomposites by colloidal technique and SPS. Ceramics International, 2020, 46, 13669-13676.	4.8	20
38	Effect of volume ratio on optical and mechanical properties of Y2O3-MgO composites fabricated by spark-plasma-sintering process. Journal of the European Ceramic Society, 2021, 41, 2096-2105.	5.7	19
39	Nanoindentation-induced plasticity in cubic zirconia up to 500°C. Acta Materialia, 2020, 184, 59-68.	7.9	18
40	Influence of spark plasma sintering conditions on microstructure, carbon contamination, and transmittance of CaF2 ceramics. Journal of the European Ceramic Society, 2022, 42, 245-257.	5.7	18
41	High-strain-rate superplastic flow in tetragonal ZrO2 polycrystal enhanced by the dispersion of 30vol.% MgAl2O4 spinel particles. Acta Materialia, 2007, 55, 4517-4526.	7.9	17
42	Strain Softening and Hardening during Superplasticâ€Like Flow in a Fineâ€Grained MgAl ₂ O ₄ Spinel Polycrystal. Journal of the American Ceramic Society, 2004, 87, 1102-1109.	3.8	15
43	Production of transparent yttrium oxide ceramics by the combination of low temperature spark plasma sintering and zinc cation-doping. Journal of the European Ceramic Society, 2018, 38, 1972-1980.	5.7	14
44	Microcrack healing in zirconia ceramics under a DC electric field/current. Journal of the European Ceramic Society, 2021, 41, 282-289.	5.7	14
45	Effect of sintering conditions on optical and mechanical properties of MgAl2O4/Al2O3 laminated transparent composite fabricated by spark-plasma-sintering (SPS) processing. Journal of the European Ceramic Society, 2022, 42, 2487-2495.	5.7	14
46	Low-temperature spark plasma sintering of alumina by using SiC molding set. Journal of the Ceramic Society of Japan, 2016, 124, 1141-1145.	1.1	12
47	Spark Plasma Sintering of Highly Transparent Hydroxyapatite Ceramics. Funtai Oyobi Fummatsu Yakin/Journal of the Japan Society of Powder and Powder Metallurgy, 2017, 64, 547-551.	0.2	12
48	Segregationâ€controlled densification and grain growth in rare earthâ€doped Y ₂ O ₃ . Journal of the American Ceramic Society, 2021, 104, 4946-4959.	3.8	12
49	Transmittance enhancement of spark plasma sintered CaF2 ceramics by preheating commercial powder. Journal of the European Ceramic Society, 2021, 41, 4609-4617.	5.7	12
50	Effect of electric current on high temperature flow behavior of 8Y-CSZ ceramics. Journal of the European Ceramic Society, 2022, 42, 2341-2348.	5.7	12
51	Effect of MgAl ₂ O ₄ Spinel Dispersion on High-Strain-Rate Superplasticity in Tetragonal ZrO ₂ Polycrystal. Materials Transactions, 2004, 45, 2073-2077.	1.2	11
52	Doping effect on the flash sintering of Y2O3: Promotion of densification and optical translucency. Journal of the European Ceramic Society, 2020, 40, 6053-6060.	5.7	11
53	Fabrication of MgAl2O4/Al2O3 laminated transparent composite by spark-plasma-sintering (SPS) processing. Scripta Materialia, 2021, 205, 114205.	5.2	11
54	Densification of Y2O3 by flash sintering under an AC electric field. Journal of the European Ceramic Society, 2022, 42, 567-575.	5.7	11

#	Article	IF	CITATIONS
55	A threshold stress for the superplastic deformation in Y2O3-stabilized tetragonal ZrO2. Materials Science & Engineering A: Structural Materials: Properties, Microstructure and Processing, 2004, 387-389, 655-658.	5.6	10
56	Grain-boundary sliding model of pore shrinkage in late intermediate sintering stage under hydrostatic pressure. Acta Materialia, 2013, 61, 6661-6669.	7.9	10
57	Fabrication and Mechanical Properties of Textured Ti ₃ SiC ₂ Systems Using Commercial Powder. Materials Transactions, 2018, 59, 829-834.	1.2	10
58	Ferroelastic and plastic behaviors in pseudo-single crystal micropillars of nontransformable tetragonal zirconia. Acta Materialia, 2021, 203, 116471.	7.9	9
59	Anelasticity induced by AC flash processing of cubic zirconia. Acta Materialia, 2022, 227, 117704.	7.9	9
60	Fracture Toughness of Yttria-Stabilized Cubic Zirconia (8Y-CSZ) Doped with Pure Silica. Materials Transactions, 2004, 45, 3324-3329.	1.2	7
61	Fabrication of Nanocrystalline Superplastic ZrO ₂ Ceramics. Materials Science Forum, 2007, 551-552, 491-496.	0.3	7
62	Simulation of densification behavior of nano-powder in final sintering stage: Effect of pore-size distribution. Journal of the European Ceramic Society, 2021, 41, 625-634.	5.7	7
63	Elastic isotropy originating from heterogeneous interlayer elastic deformation in a Ti3SiC2 MAX phase with a nanolayered crystal structure. Journal of the European Ceramic Society, 2021, 41, 2278-2289.	5.7	7
64	High-Strain-Rate Superplasticity in 3mol%-Y ₂ O ₃ -Stabilized Tetragonal ZrO ₂ Dispersed with 30vol% MgAl ₂ O ₄ Spinel. Materials Science Forum, 2004, 447-448, 329-334.	0.3	6
65	Shrinkage of Pores Located at Grain Corners by Grain-Boundary Diffusion. Journal of the American Ceramic Society, 2011, 94, 982-984.	3.8	6
66	Nano ZrO ₂ –TiN composites with high strength and conductivity. Journal of the Ceramic Society of Japan, 2015, 123, 86-89.	1.1	6
67	Theoretical analysis of experimental densification kinetics in final sintering stage of nano-sized zirconia. Journal of the European Ceramic Society, 2019, 39, 1359-1365.	5.7	6
68	Experimental confirmation of the symmetric sintering behavior under compressive/tensile loading combined with electrical field. Scripta Materialia, 2020, 187, 137-141.	5.2	6
69	Effect of the Heating Rate on the Spark-Plasma-Sintering (SPS) of Transparent Y2O3 Ceramics: Microstructural Evolution, Mechanical and Optical Properties. Ceramics, 2021, 4, 56-69.	2.6	6
70	Microstructural examination in high-strain-rate superplastically deformed tetragonal ZrO2 dispersed with 30 vol% MgAl2O4 spinel. Journal of Materials Research, 2007, 22, 801-813.	2.6	5
71	Evaluation of densification and grain-growth behavior during isothermal sintering of zirconia. Journal of the Ceramic Society of Japan, 2017, 125, 357-363.	1.1	3
72	Fabrication of Textured Porous Ti ₃ SiC ₂ by Slip Casting under High Magnetic Field and Microstructural Evolution through High Temperature Deformation. Nippon Kinzoku Gakkaishi/Journal of the Japan Institute of Metals, 2021, 85, 256-263.	0.4	3

#	Article	IF	CITATIONS
73	Fabrication of Textured Porous Ti ₃ SiC ₂ by Slip Casting under High Magnetic Field and Microstructural Evolution through High Temperature Deformation. Materials Transactions, 2022, 63, 133-140.	1.2	3
74	Development of High-Strain-Rate Superplastic Oxide Ceramics Based on Flow Mechanism. Materials Science Forum, 2012, 735, 9-14.	0.3	2
75	Fabrication and Mechanical Properties of Textured Ti ₃ SiC ₂ MAX Phase Systems. Funtai Oyobi Fummatsu Yakin/Journal of the Japan Society of Powder and Powder Metallurgy, 2016, 63, 970-975.	0.2	2
76	Micro-Crack Healing in Cubic Zirconia (8Y-CSZ) Using Flash Event. Nippon Kinzoku Gakkaishi/Journal of the Japan Institute of Metals, 2022, 86, 23-29.	0.4	2
77	High-Strain-Rate Superplastic Flow Mechanism in ZrO ₂ -30vol% Spinel Two-Phase Composite. Key Engineering Materials, 2010, 433, 333-338.	0.4	1
78	Densification Mechanism of MgAl ₂ O ₄ Spinel during Spark-Plasma-Sintering. Advances in Science and Technology, 2010, 63, 62-67.	0.2	1
79	Fabrication of Transparent Ceramic Polycrystals by means of Spark-Plasma-Sintering (SPS) Technique. Materia Japan, 2014, 53, 3-10.	0.1	1
80	Fabrication of Dense Nanostructured Bulk Ceramics by Means of Spark-Plasma-Sintering (SPS) Processing. Materials Science Forum, 2016, 838-839, 225-230.	0.3	1
81	Strong Field-induced Nanodynamics in Ceramics. Materia Japan, 2021, 60, 19-24.	0.1	1
82	Orientation Dependence of Plastic Deformation Behavior and Fracture Energy Absorption Mechanism around Vickers Indentation of Textured Ti ₃ SiC ₂ Sintered Body. Funtai Oyobi Fummatsu Yakin/Journal of the Japan Society of Powder and Powder Metallurgy, 2020, 67, 607-614.	0.2	1
83	Electrode overvoltage model for a flash state of yttria-stabilized zirconia: validity, limitation, and open new issue. Journal of the Ceramic Society of Japan, 2022, 130, 172-179.	1.1	1
84	Role of Deformable Fine Spinel Particles in High-Strain-Rate Superplastic Flow of Tetragonal ZrO2. Materials Research Society Symposia Proceedings, 2004, 821, 288.	0.1	0
85	Mechanical Properties of Textured Alumina Prepared by Colloidal Processing in a Strong Magnetic Field. Materials Research Society Symposia Proceedings, 2006, 977, 1.	0.1	0
86	Densification Behavior in Spark-Plasma-Sintering of MgAl ₂ O ₄ Spinel. Materials Science Forum, 2010, 654-656, 1986-1989.	0.3	0
87	YMnO3-ZnO Thermoelectrics. Zeitschrift Fur Anorganische Und Allgemeine Chemie, 2012, 638, 1630-1630.	1.2	0
88	Influence of Loading Condition on Fabrication of Transparent MgAl ₂ O ₄ Spinel Ceramics by Spark-Plasma-Sintering (SPS) Technique. Funtai Oyobi Fummatsu Yakin/Journal of the Japan Society of Powder and Powder Metallurgy, 2014, 61, 565-574.	0.2	0
89	Fabrication and Mechanical Properties of Textured Ti ₃ SiC ₂ Systems Using Commercial Powders. Funtai Oyobi Fummatsu Yakin/Journal of the Japan Society of Powder and Powder Metallurgy, 2017, 64, 552-557.	0.2	0
90	Possibility of Low-Temperature High-Strain-Rate Superplasticity in Fine-Grained Ceramic Materials. Funtai Oyobi Fummatsu Yakin/Journal of the Japan Society of Powder and Powder Metallurgy, 2017, 64, 515-522.	0.2	0

#	Article	IF	CITATIONS
91	Fabrication of Transparent Polycrystalline Ceramics by Utilizing External Field Effects. Funtai Oyobi Fummatsu Yakin/Journal of the Japan Society of Powder and Powder Metallurgy, 2019, 66, 158-167.	0.2	Ο
92	Atomic Structure of ‹001› <i>Σ</i> 5 Asymmetric Tilt Boundary in Molybdenum. Materia Japan, 2006, 45, 843-843.	0.1	0
93	Development of Laser Optical Elements by Spark Plasma Sintering Technique. The Review of Laser Engineering, 2019, 47, 448.	0.0	0
94	Development of Laser Optical Materials by Pulsed Electric Current Sintering. Funtai Oyobi Fummatsu Yakin/Journal of the Japan Society of Powder and Powder Metallurgy, 2021, 68, 476-481.	0.2	0
95	Effect of Powder Calcination Conditions on IR Transmission in Y ₂ O ₃ -MgO Nanocomposites Fabricated by Pulsed Electric Current Sintering Technique. Funtai Oyobi Fummatsu Yakin/Journal of the Japan Society of Powder and Powder Metallurgy, 2021, 68, 500-506.	0.2	0